Chinese Chemical Letters 37 (2026) 111773

Contents lists available at ScienceDirect

Chinese Chemical Letters

journal homepage: www.elsevier.com/locate/cclet

Discovery of marine-derived *ent*–atisane diterpenoid lead compounds targeting sEH for Alzheimer's disease therapy

Fan Yang[a,1], Tingting Fu[a,b,1], Wandi Xiong[a,1], Shuting Zhang[a], Junjie Wang[a], Wenjun Shan[c], Xinyi Chen[a], Mingbin Chen[a], Qi Guo[a,d], Jinzhuo Li[a,d], Junyi Li[a], Jingru Liu[a], Jin Liu[a], Yong Rao[a], Zhongping Jiang[a,*], Congjun Xu[a,*], Ling Huang[a,*]

[a] *Key Laboratory of Tropical Biological Resources of Ministry of Education, School of Pharmaceutical Sciences, Hainan University, Haikou 570228, China*
[b] *NHC Key Laboratory of Tropical Disease Control, School of Tropical Medicine School of Pharmaceutical Sciences, Hainan Medical University, Haikou 571199, China*
[c] *Shanghai Haiyan Pharmaceutical Technology Co., Ltd., Shanghai 201203, China*
[d] *School of Pharmaceutical Engineering, Shenyang Pharmaceutical University, Shenyang 110016, China*

ARTICLE INFO

Article history:
Received 24 July 2025
Revised 28 August 2025
Accepted 29 August 2025
Available online 29 August 2025

Keywords:
sEH inhibitor
Marine
Natural products
Diterpenoid
Alzheimer's disease

ABSTRACT

Accumulating evidence highlights the therapeutic potential of soluble epoxide hydrolase (sEH) inhibitors with anti-inflammatory and neuroprotective properties for Alzheimer's disease (AD). In this work, an *ent*–atisane diterpenoid **J12** was identified as a hit compound against sEH with moderate inhibitory activity from five distinct series of compounds (**J1**–**J44**) isolated from *Excoecaria agallocha* L. After rational structural modification, a novel sEH inhibitor HXY14 with improved sEH inhibitory activity (half maximal inhibitory concentration (IC_{50}) = 1.6 μmol/L, 10-fold compared to **J12**) was obtained. The cellular thermal shift assay (CETSA) demonstrated direct binding of HXY14 to sEH. In an Aβ-induced neuroinflammation cell model, treatment with HXY14 increased epoxyeicosatrienoic acids (EETs) levels, leading to reduced neuroinflammation and concomitant neuroprotection. HXY14 could ameliorate memory impairment and exhibited cognitive improvement in $A\beta_{1-42}$-induced AD model and exhibited preferable safety *in vivo*. Treatment with HXY14 significantly decreased the expression levels of inflammatory factors and attenuated microglia activation, thereby inhibiting neuroinflammation. Furthermore, HXY14 could promote neuroprotection and alleviate synaptic dysfunction in AD model mice. This study expands the discovery of novel naturally derived sEH inhibitors and provides evidence for the utility of sEH inhibitors for AD therapy.

© 2026 Published by Elsevier B.V. on behalf of Chinese Chemical Society and Institute of Materia Medica, Chinese Academy of Medical Sciences.

Alzheimer's disease (AD), the most common neurodegenerative disorder and leading course of dementia, is characterized by progressive memory loss, cognitive decline, disorientation, and loss of functional independence [1–3], posing escalating socioeconomic burdens on healthcare systems globally [4]. The pathogenesis of AD is multifactorial, encompassing the accumulation of amyloid plaques, tau hyperphosphorylation, cholinergic dysfunction, neuroinflammation, oxidative stress, microbiota-gut-brain axis, and other contributing factors [5–8], all of which collectively inform the development of therapeutic strategies [9–11]. Current pharmacological management of AD primarily involves acetylcholinesterase (AChE) inhibitors and *N*-methyl-D-aspartic acid (NMDA) receptor antagonists, which provide symptomatic relief for cognitive impairments while demonstrating significant adverse effect profiles [12]. Emerging disease-modifying therapies (DMTs) targeting Aβ protein, including aducanumab and lecanemab, demonstrate potential to modify AD progression, yet their safety and efficacy require further evaluation [13,14]. In summary, available medications still do not meet the needs of AD patients.

Currently, neuroinflammation has emerged as a critical etiological factor in AD [15]. Central nervous system (CNS)-resident cells (*e.g.*, microglia, astrocytes) and regulatory molecules (*e.g.*, cytokines, chemokines) involved in neuroinflammation are implicated in various aspects of AD pathology, causing or exacerbating cognitive decline [16,17]. Soluble epoxide hydrolase (sEH) is a key enzyme involved in inflammatory pathways [18,19] that converts anti-inflammatory epoxyeicosatrienoic acids (EETs) to pro-inflammatory dihydroxyeicosatrienoic acids (DHETs) [20]. Accumulating evidence indicated that sEH inhibition effectively maintains

* Corresponding authors.
E-mail addresses: zpjiang@hainanu.edu.cn (Z. Jiang), congjunxu@hainanu.edu.cn (C. Xu), Linghuang@hainanu.edu.cn (L. Huang).
[1] These authors contributed equally to this work.

https://doi.org/10.1016/j.cclet.2025.111773
1001-8417/© 2026 Published by Elsevier B.V. on behalf of Chinese Chemical Society and Institute of Materia Medica, Chinese Academy of Medical Sciences.

endogenous levels of EETs, leading to a significant reduction in inflammation [21–23]. Since sEH is abundantly expressed throughout various brain regions, the neuroprotective effects of sEH inhibitors have emerged as a promising research focus in the treatment of CNS disorders [24]. Numerous studies have demonstrated that sEH exhibits significant overexpression in both AD mouse models and human AD brains compared with healthy controls, further supporting its association with AD pathogenesis [25,26]. sEH deficiency has been shown to mitigate Aβ deposition, enhance anti-inflammatory cytokine production (interleukin-4 (IL-4)/IL-10), suppress nuclear factor kappa-B (NF-κB) signaling, and ameliorate behavioral deficits in *APP/PS1 Tg* mice [27]. In parallel, 5XFAD mice treated with the sEH inhibitor 1-trifluoromethoxyphenyl-3-(1-propionylpiperidin-4-yl) urea (TPPU) (Fig. S1 in Supporting information) attenuated neuroinflammation, reduced amyloid pathology, and rescued cognitive decline [28]. Up to now, the development of sEH inhibitors presents a novel therapeutic strategy for current AD treatment.

To date, only three sEH inhibitors (AR9281 [29], GSK2256294 [30], and EC5026 [31]) have advanced to human clinical trials, with their therapeutic efficacy remaining to be fully validated. Although inhibition of sEH represents a promising strategy for AD therapy, the scarcity of clinically approved sEH inhibitors underscores the necessity for developing novel inhibitor scaffolds. Natural products (NPs) play a pivotal role in AD drug discovery due to their diverse biological activities [32,33]. Numerous compounds derived from NPs, including natural ureas, triterpenoids, flavonoids, and phenylpropanoids, have been reported to show inhibitory effects on sEH [34–36]. However, their therapeutic utility is limited by suboptimal potency and insufficient *in vivo* validation. Our prior investigation identified diterpenoid NPs [37,38] derived from the mangrove plant *Excoecaria agallocha* L. that exhibit potent anti-neuroinflammatory activity, providing a structural foundation for AD drug discovery efforts. In this study, through systematic bioactivity screening and structural optimization of *ent*–atisane diterpenoid compounds derived from *Excoecaria agallocha* L., we have discovered a series of novel sEH inhibitors with previously unreported structural scaffolds. *In vivo* therapeutic evaluation in AD model mice and mechanism exploration were also performed. The results demonstrated that mangrove-derived *ent*–atisane diterpenoid sEH inhibitors exhibit promising therapeutic potential for alleviating neuroinflammation and ameliorating cognitive deficits in AD.

We isolated and identified five series of compounds characterized by diterpenoid hydrophobic scaffolds from the mangrove plant *Excoecaria agallocha* L. (Scheme S1 in Supporting information). It is noteworthy that the majority of diterpenoid NPs demonstrate acceptable anti-neuroinflammatory activity, holding decent potential as lead compounds for CNS drug development [38,39]. In parallel, numerous investigational sEH inhibitors have highlighted the critical role of hydrophobic moieties such as adamantane and substituted aryl groups in their inhibitory activity [40–42], which fit neatly with the structural features of diterpenoids. In this work, given their notable anti-inflammatory activity and hydrophobic scaffolds, we screened 44 *Excoecaria agallocha* L.-derived compounds for their inhibitory effects on sEH *in vitro* through recombinant human sEH (HsEH) inhibitory enzymatic assays. As shown in Fig. S2 (Supporting information), none of the *ent*–isopimaranes (**J27**–**J34**) exhibited detectable sEH inhibitory activity. In contrast, the other four classes of diterpenoids demonstrated sEH inhibition to varying extents. Among these, the *ent*–atisane type diterpenoids (**J1**–**J17**) displayed relatively higher activity, with **J12** emerging as the most potent sEH inhibitor. Among the *ent*–atisanes diterpenoid derivatives, a significant enhancement in biological activity was observed when the carboxylic acid moiety (compound **J10**) was substituted with an ester functional group (compound **J3**). These findings indicated that modification of the carboxylic acid moiety may play a pivotal role in optimizing the pharmacophore configuration, potentially modulating target binding affinity. Moreover, the binding pattern of the compounds to sEH similarly supports the finding above.

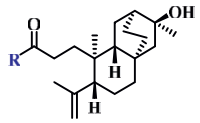
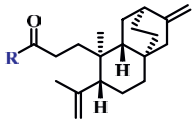
Molecular docking was performed to investigate the potential mechanisms underlying the interaction between *ent*–atisane diterpenoid (optimal compound **J12**) and sEH protein (PDB ID: 3WKE, crystal structure of sEH in complex with *t*-AUCB). As shown in Fig. S3 (Supporting information), the diterpenoid core of the compound **J12** occupies the hydrophobic pocket, establishing π-π stacking interactions with relevant aromatic residues, such as MET-419. While the carbonyl group forms a hydrogen bond with the catalytic residue TYR-466. Both structural features are essential for sEH inhibitory activity, consistent with prior literature reports [43,44], which collectively accounts for the moderate sEH inhibitory activity. Notably, the carboxyl group was oriented toward the larger L-shaped hydrophobic pocket, allowing the introduction of polar functional groups to improve the binding efficacy and physicochemical properties. Inspired by these findings, NP **J12** was selected as hit compound and systematically modified, culminating in a series of novel *ent*–atisane diterpenoid-derived sEH inhibitors with optimized pharmacophores.

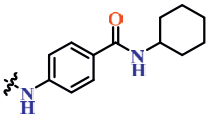
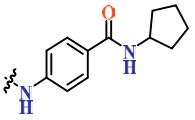
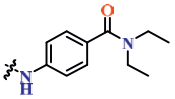
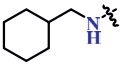
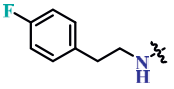
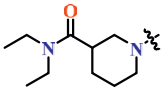
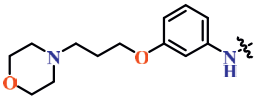
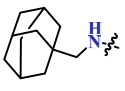
To further explore the sEH inhibitory potential of *ent-atisane* diterpenoid, structural optimization was performed in this study. Inspired by the findings above, the carboxylic acid group of diterpenoid derivatives was replaced with amide moieties commonly found in sEH inhibitors, while novel or previously reported polar functional groups [24] were strategically incorporated. The activities of target compounds against HsEH were evaluated with the hit compound **J12** and the previously reported NPs-derived sEH inhibitor kaempferol [36] as controls. As described in Table 1, structural modifications to **J10** (18.6 % ± 1.6 %) resulted in enhanced inhibitory activity, consistent with preliminary SARs, thereby confirming the viability of the design strategy. Moreover, compounds HXY5 and HXY6 incorporating cyclopentyl and cyclohexyl moieties exhibited better inhibitory potency, suggesting that bulky hydrophobic substituents played a substantial role in potency.

Building on this, hydrophobic cycloalkanes and aryl groups were introduced into the hit compound **J12** (half maximal inhibitory concentration (IC_{50}) = 14.8 μmol/L), with the aryl derivatives exhibiting promising activity (HXY12). Thereafter, amide pharmacophores and alkyl termini were introduced while retaining the aryl linker, with concomitant retention of activity (HXY7–9). Subsequently, to further diversify the scaffold, a piperidine moiety and reported optimal flexible group were introduced, which afforded a marked enhancement in activity. Notably, compound HXY14 (IC_{50} = 1.6 μmol/L) incorporating both aryl ether and morpholine moieties, exhibited enhanced sEH inhibitory activity. We postulate that the aryl group and flexible carbon chain facilitate adoption of a more productive binding pose with the target, as confirmed in molecular docking studies (Fig. 1). Collectively, the *Excoecaria agallocha* L.-derived diterpenoid scaffold demonstrated high structural versatility, providing a privileged template for the development of novel sEH inhibitors. In addition, HXY14 demonstrated blood-brain barrier permeability with a permeability coefficient (Pe) of 2.8 ± 0.11. Therefore, considering all factors, we chose HXY14 for the subsequent activity evaluation.

To assess the potential impact of HXY14 on cell viability, we first conducted drug toxicity tests on N2a, BV2, and C8-D1A cell lines. Based on the results by CCK8 assays, the results showed that HXY14 exhibited minimal biological toxicity to different neuronal cells (Figs. 1A–C). To further validate the targeting between sEH inhibitors HXY14 and sEH protein, we performed molecular docking analysis and cellular thermal shift assay (CETSA). Molecular docking experiments were used to investigate possible binding modes

Table 1
In vitro biological activity of *Excoecaria agallocha* L. derivatives against HsEH.

Entry	Series	R	sEH% inhibition at 10 μmol/L[b]	sEH% inhibition at 1 μmol/L	IC_{50} (μmol/L)	Pe ($\times 10^{-6}$ cm/s)[d]
J10	A		18.6 ± 1.6[c]	-	NT	0.25 ± 0.07
HXY1	A		26.3 ± 1.0	NT[a]	NT	NT
HXY2	A		19.1 ± 4.8	NT	NT	NT
HXY3	A		32.2 ± 7.1	NT	NT	NT
HXY4	A		16.7 ± 6.3	NT	NT	NT
HXY5	A		44 ± 2.5	NT	NT	NT
HXY6	A		57.3 ± 7.7	NT	NT	NT
J12	B		43.8 ± 4.9	-	14.8 ± 1.0	0.31 ± 0.11
HXY7	B		49.6 ± 4.6	NT	NT	NT
HXY8	B		14.9 ± 8.3	NT	NT	NT
HXY9	B		15.4 ± 9.8	NT	NT	NT
HXY10	B		39.3 ± 2.9	18.5 ± 1.6	NT	NT
HXY11	B		37.4 ± 2.4	−3.2 ± 3.5	NT	NT
HXY12	B		48.6 ± 2.3	17.5 ± 4.9	NT	NT
HXY13	B		75.1 ± 7.6	0.4 ± 1.6	6.0 ± 0.2	2.3 ± 0.71
HXY14	B		68.4 ± 1.8	32.9 ± 0.8	1.6 ± 0.1	2.8 ± 0.11
HXY15	B		21.5 ± 7.4	18.1 ± 7.2	NT	NT
Kaempferol					8.5 ± 0.3	NT

[a] No test.
[b] Results are the mean of three independent experiments ($n = 2$).
[c] Standard deviation.
[d] Results are the mean of three independent experiments ($n = 3$) ± standard deviation. Compounds have low blood-brain barrier permeation when Pe < 1.8×10^{-6} cm/s.

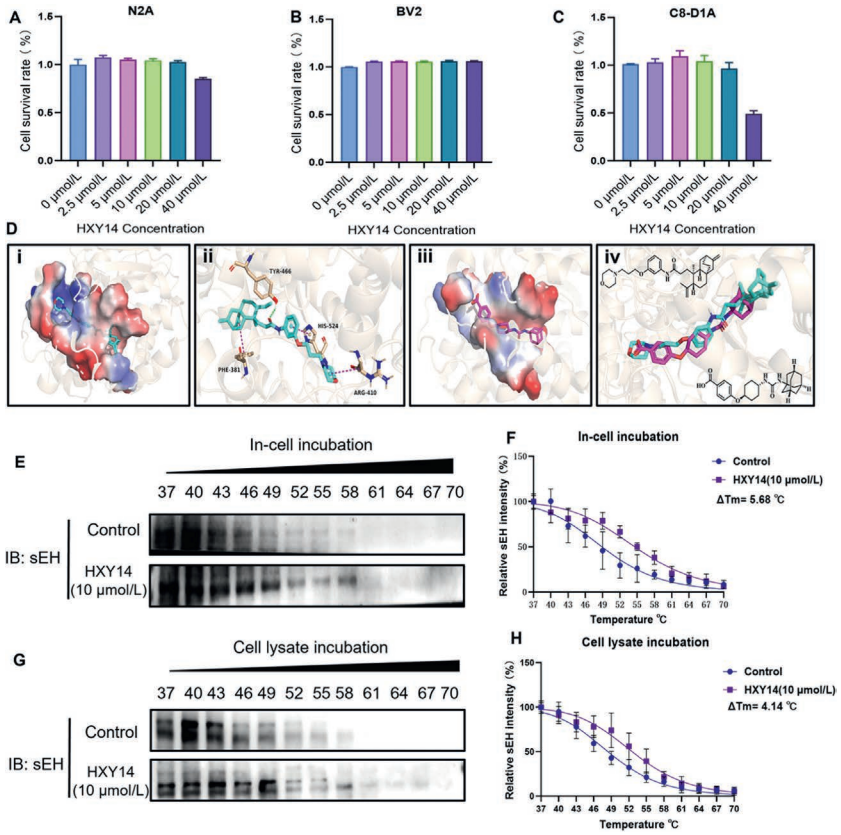


Fig. 1. HXY14 binds to sEH. (A–C) Cell viability assay after co-incubation of N2a, BV2, and C8-D1A cells with different concentrations of HXY14. (D) Docking analysis of HXY14 bound to sEH (PDB ID: 3WKE). (i) Docked poses of HXY14. (ii) Interaction map between HXY14 and binding sites. (iii) The crystal structure of the sEH enzymatic pocket with bound sEHI, *trans*-4-[4-(3-adamantan-1-yl-ureido)-cyclohexyloxy]-benzoic acid (*t*-AUCB). (iv) Comparison of the binding poses of HXY14 (cyan) and *t*-AUCB (purple). (E) WB validation results of the CETSA assay sample after in-cell incubation. IB, immunoblotting. (F) Analysis of relative grey values of WB validation results of CETSA assay sample after in-cell incubation. (G) WB validation results of CETSA assay sample after cell lysate incubation. (H) Analysis of relative grey values of WB validation results of CETSA assay sample after cell lysate incubation. Error bars signify mean ± SEM ($n = 3$–5 per group).

of representative compound HXY14 in the pocket of sEH protein (PDB ID: 3WKE). Visualization was performed in PyMOL (v2.5.0). As illustrated in Fig. 1D, the polar groups introduced in HXY14 successfully penetrated the protein cavity, which facilitates ligand-receptor binding. The diterpene skeleton resides within the hydrophobic pocket while retaining the hydrogen bond between its carbonyl group and residues TYR-466. Furthermore, the newly introduced phenyl ring and morpholine group establish π-π stacking interactions with residues HIS-524 and ARG-410. Those results demonstrate that HXY14 adopts a consistent binding pose with the sEH inhibitor *t*-AUCB: The diterpene scaffold mimics the spatial contribution of the adamantane group in *t*-AUCB, while the amide moiety functions analogously to the urea group. This binding mode rationalizes the compound's observed sEH inhibitory activity. The CETSA results showed that, compared with the control group, in cell lysate incubation, the sEH protein treated with HXY14 had better thermal stability and slowed down their degradation (Figs. 1E–H). Taken together, the results suggest that HXY14 may directly bind to sEH protein.

The EETs are synthesized from arachidonic acids by cytochrome P450 and hydrolyzed by sEH, which contributes to anti-inflammatory activity. Here, to investigate whether HXY14 exerts protective effects on Aβ_{1-42}-induced cell model, which is regarded as a common AD cell model, we measured the EETs levels from the experimental group. As shown in Fig. S4 (Supporting information), they are showed significantly lower levels in Aβ_{1-42}-induced BV2 cell group but were rescued in the groups treated with the 2 and 10 μmol/L HXY14, and sEH inhibitors kaempferol and TPPU (Fig. S4A). To further investigate the anti-neuroinflammatory effects of HXY14 in AD conditions, we detected the mRNA levels of several major inflammatory factors, including NF-κB, IL-6, and cyclooxygenase-2 (COX2) (Figs. S4B–D). The RT-qPCR results exhibited that 2 and 10 μmol/L HXY14 inhibited the mRNAs expression levels of NF-κB, IL-6, and COX2 in Aβ_{1-42}-induced BV2 cells, which is consistent with the groups treated sEH inhibitors kaempferol and TPPU. Further combined with an immunofluorescence assay, we also found that Aβ_{1-42}-induced an increase of inducible nitric oxide synthase (iNOS) expression (Figs. S4E and F). Both HXY14 and sEH inhibitors kaempferol and TPPU significantly inhibited iNOS expression levels. Furthermore, the supernatants from Aβ_{1-42}-induced BV2 cells treated with HXY14 and sEH inhibitors kaempferol and TPPU were cultured with N2a cells. The results showed that these supernatants significantly increased brain-derived neurotrophic factor (BDNF) expression (Figs. S4G and H). These results suggest that HXY14 relieves neuroinflammatory effects and further increases the actions on neuroprotection.

To investigate the therapeutic effects of *Excoecaria agallocha* L.-derived sEH inhibitors on AD, we conducted a series of behavioral tests, including open field test (OFT), object recognition test (ORT) and Morris water maze test (MWM), followed by biochemical experiments to explore the underlying mechanisms. All animal experiments were approved by the Ethics Committee of Hainan University (approval No. HPIACUC2024141). The Aβ_{1-42} stereotactic injection model was established to test the effect of compound HXY14 on cognitive function in AD model. The behavioral tests were conducted in chronological order after 2 weeks of treatment

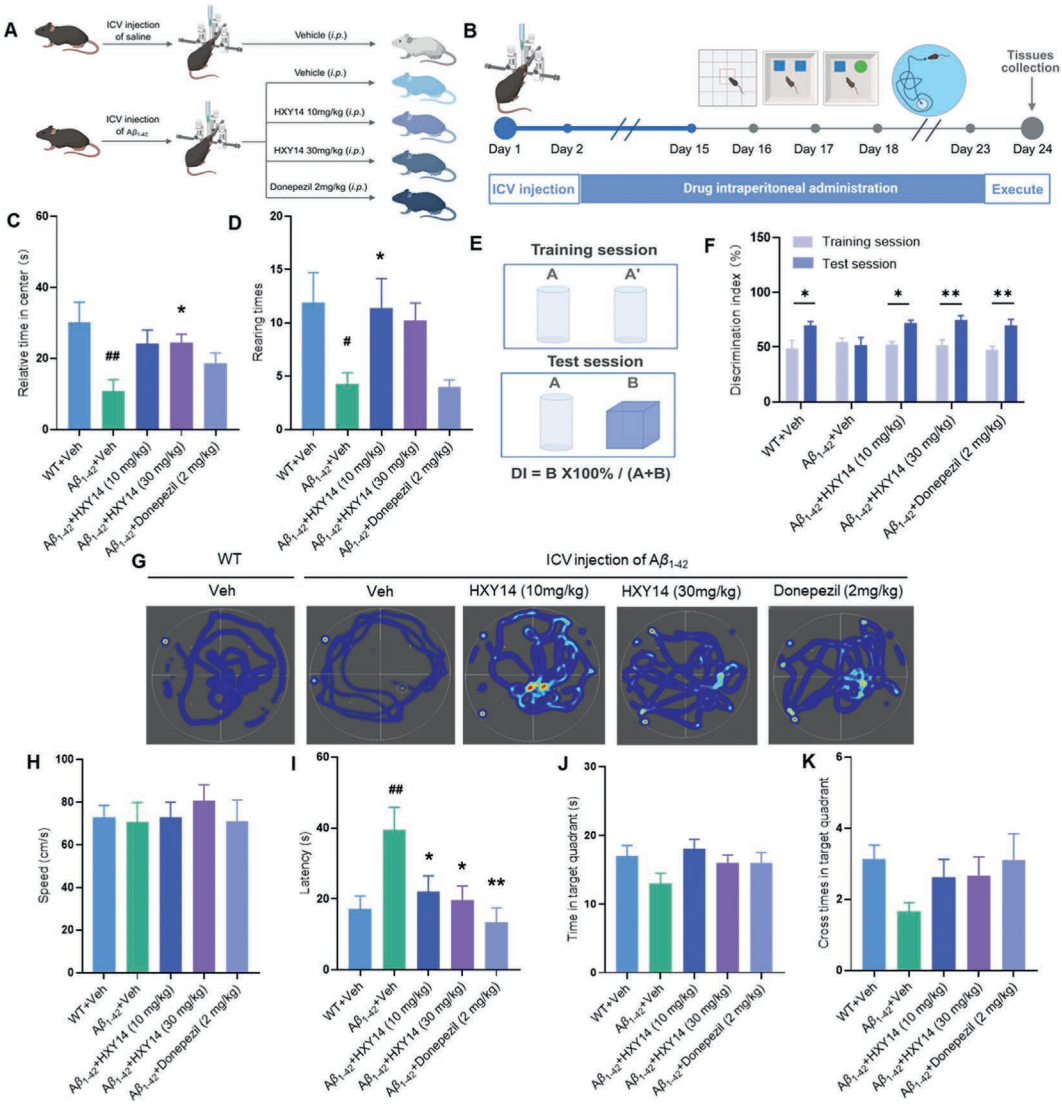


Fig. 2. HXY14 showed cognitive improvement in AD model. (A) Schematic diagram of experimental design. (B) Timeline demonstrating the chronological order of behavioral tests after HXY14 treatment. (C) Time in center of each group in the OFT. (D) Rearing times of each group in the OFT. (E) Schematic diagram of the ORT. (F) DI of each group in the ORT. (G) Representative swimming trace of each group in the MWM test. (H) Swimming speed of each group in the MWM test. (I) Escape latency time of each group in the spatial probe trial. (J) Accumulated time in target quadrant of each group in MWM test. (K) Frequency of the hidden platform site crossings of each group in MWM test. Error bars signify mean ± SEM ($n = 9$–11 animals per group). $^{\#}P < 0.05$, $^{\#\#}P < 0.01$ *vs.* control; $^{*}P < 0.05$, $^{**}P < 0.01$ *vs.* model.

with vehicle, preferred compound HXY14 (10.0 and 30.0 mg/kg, *i.p.*), and Donepezil (2.0 mg/kg, *i.p.*) (Figs. 2A and B).

During the OFT session, Aβ_{1-42} administration mice treated with compound HXY14 exhibited good performance with more time in the center region and more times of rearing behavior (Figs. 2C and D). During the ORT session, Aβ_{1-42}-administration mice treated with compound HXY14 showed increased discrimination index (DI) (Figs. 2E and F). During the MWM training session, mice treated with compound HXY14 exhibited a significantly decreased latency time to locate the hidden platform without any effect on swimming speed (Figs. 2G–I). During the spatial probe test of the MWM, the HXY14-treated group exhibited increased cross times and time in the target quadrant compared to the Aβ_{1-42} administration group (Figs. 2J and K). In summary, behavioral tests demonstrate that the compound HXY14 ameliorated memory impairment and exhibited cognitive improvement in AD, suggesting it might thus be a novel anti-AD agent.

Furthermore, as shown in Fig. S5 (Supporting information), the treatment with compound HXY14 for 2 weeks had no effect on the mean daily bodyweight profile in mice (Fig. S5A). The liver function and kidney function were evaluated by testing the biochemical indicators of the serum. The serum indicators, including total bilirubin (T-Bil), alanine aminotransferase (ALT), aspartate transaminase (AST), creatinine (CREA), carbonyl diamide (UREA), and AST/ALT ratio, showed a normal range in all experimental groups (Fig. S5B). The morphological examination of the mice hippocampus was performed by hematoxylin-eosin (H&E) staining. The number of neurons and morphology of nuclei exhibited no evident abnormality in cornu ammonis area 1 (CA1), CA3, and dentate gyru (DG) areas in hippocampus from all these groups (Figs. S5C–F). Taken together, HXY14 showed no significant toxicity in Aβ_{1-42} administration mice and caused minimal damage to hippocampal neurons. sEH inhibition has been proposed as a potential intervention for reducing the chronic neuroinflammation in neurodegenerative disease. AD is characterized for Aβ accumulation, which could result in microglia activation and neuroinflammation. sEH inhibitors are reported to have anti-inflammatory and neuroprotective effects for the treatment of AD. In our study,

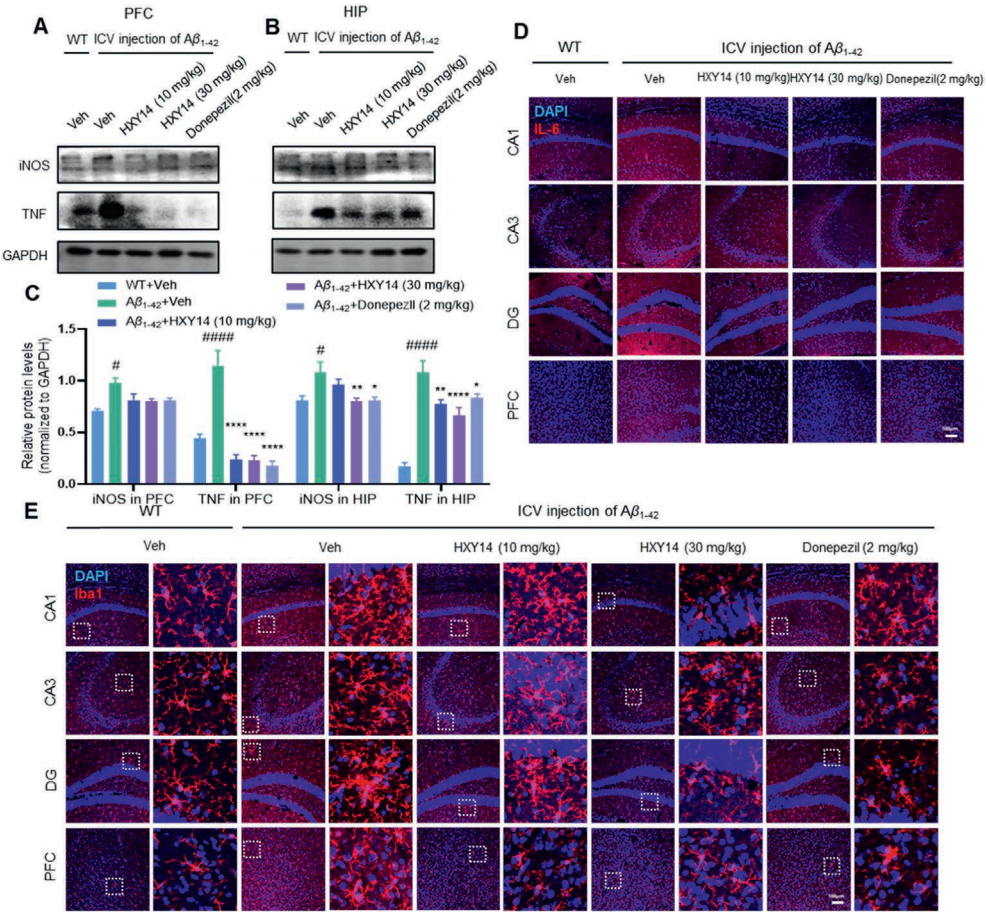


Fig. 3. HXY14 attenuates neuroinflammation and microglia activation in AD mice. Protein expression of iNOS and TNF in PFC (A) and hippocampus (B) regions was detected by WB. ICV, intra-cerebroventricular injection; WT, wild type; GAPDH, glyceraldehyde-3-phosphate dehydrogenase. (C) Quantification of the relative intensities of iNOS and TNF in PFC and hippocampus. (D) The immunofluorescence analysis of IL-6 in CA1, CA3, DG, and PFC regions of each group. DAPI, 4′,6-diamidino-2-phenylindole. (E) The immunofluorescence analysis of Iba1 in CA1, CA3, DG, and PFC regions of each group. Scale bar: 100 μm. Error bars signify mean ± SEM ($n = 4$–6 animals per group). $^{\#}P < 0.05$, $^{\#\#\#\#}P < 0.0001$ *vs.* control; $^{*}P < 0.05$, $^{**}P < 0.01$, $^{****}P < 0.0001$ *vs.* model.

treatment with HXY14 in Aβ_{1-42}-induced AD model significantly decreased the expression levels of inflammatory factors, such as iNOS and tumor necrosis factor (TNF), in both prefrontal cortex and hippocampus regions (Figs. 3A–C). The immunofluorescence results demonstrated that HXY14 treatment decreased the IL-6 distribution in CA1, CA3, DG, and prefrontal cortex (PFC) regions, while Donepezil group showed little decreasing tendency (Fig. 3D). Meanwhile, to evaluate the inflammatory damage to microglia activation, we labeled the microglia with Iba1 marker. Aβ_{1-42}-induced AD model exhibited amoeboid morphology with hypertrophy soma, resulting in a polarization to pro-inflammatory phenotype that expresses iNOS. Subsequently, sEH inhibitor treatment with compound HXY14 in high-dose group significantly alleviated morphological alteration of microglia in CA1, CA3, DG, and PFC regions (Fig. 3E). These findings indicated that sEH inhibitor HXY14 could attenuate neuroinflammation and microglia activation in AD mice, which further plays an essential role in the cognitive improvements for the treatment of AD.

The interplay between microglia activation and inflammation-associated disturbances could further affect synaptic function. It has been well-established that synaptic dysfunction impairs the long-term potentiation, and subsequently affects cognitive function and behavior. The impaired cognitive functions are the primary manifestation of neuronal dysfunction in AD. The synaptic plasticity is indicated by a pre-synaptic marker synapsin I and a post-synaptic marker PSD95. We assessed synaptic plasticity-related proteins, including synapsin I and PSD95 by Western blot (WB) and immunofluorescence. In WB, the levels of synapsin I and PSD95 in PFC and hippocampus regions decreased in Aβ_{1-42}-induced AD mice compared with WT group but rescued in HXY14 high-dose group (Figs. 4A–C). Immunofluorescence further showed that the level of synapsin I and PSD95 was significantly decreased in CA1, CA3, and DG except PFC region of AD model group compared with WT group and increased in HXY14-treated mice (Figs. 4D–G). These findings indicated that HXY14 could promote neuroprotection and alleviate synaptic dysfunction in AD mice.

In summary, an *ent*–atisane diterpenoid **J12** with attractive scaffolds was initially identified as hit compound based on a recombinant sEH inhibitory enzymatic assay from five different types of mangrove species *Excoecaria agallocha* L.-derived compounds (**J1**–**J44**). Inspired by preliminary SARs and binding pattern analyses, several novel derivatives with unreported diterpene scaffolds were further designed and synthesized based on hit compound **J12**, resulting in an effective lead compound HXY14 with 10-fold improvement compared with the hit compound. In addition, HXY14 demonstrated blood-brain barrier permeability with a Pe of 2.8 ± 0.11. Molecule docking studies demonstrated that HXY14 adopts a consistent binding pose with reference sEH inhibitor, and CETSA experiment confirmed the potent sEH binding affinity of compound HXY14. Furthermore, in an Aβ-induced BV2 cellular model of neuroinflammation, HXY14 treatment significantly increased EETs levels and suppressed the expression of key

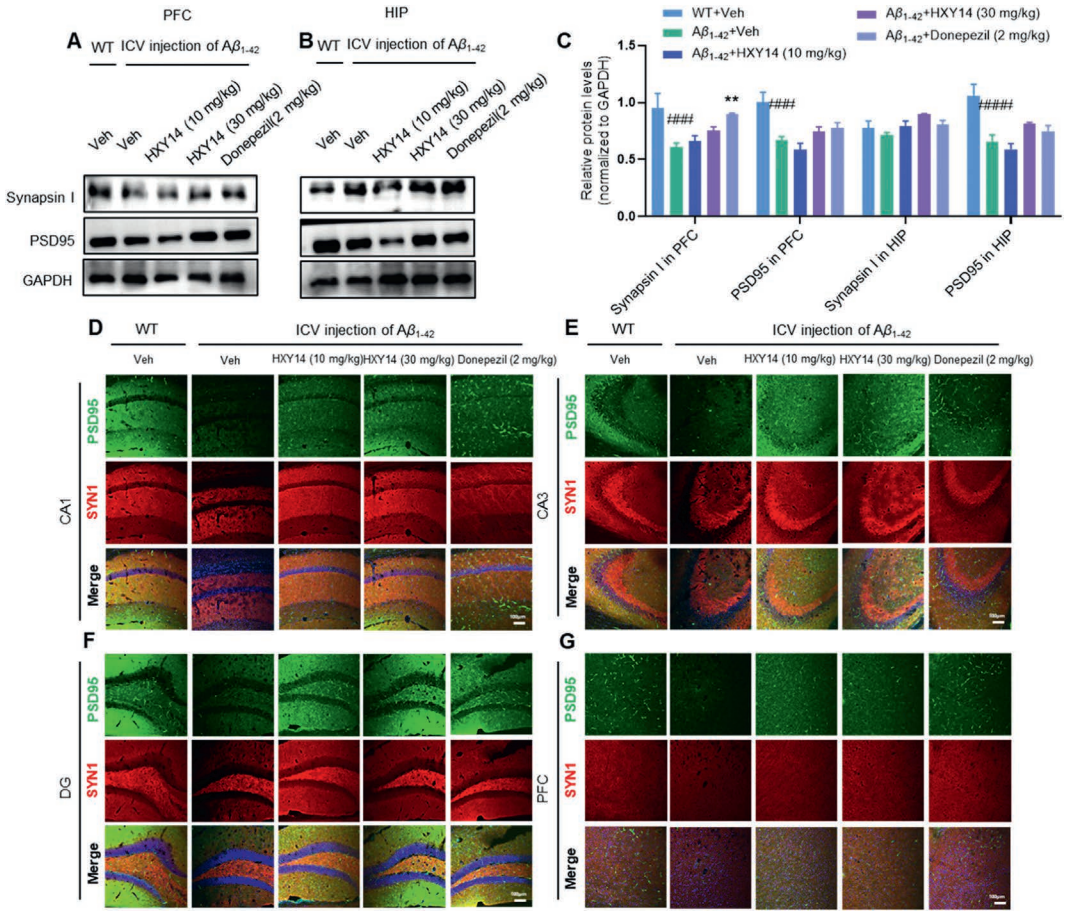


Fig. 4. HXY14 alleviates synaptic dysfunction in AD mice. Protein expression of synapsin I and PSD95 in PFC (A) and hippocampus (B) region was detected by WB. (C) Quantification of the relative intensities of synapsin I and PSD95 in PFC and hippocampus. (D–G) The immunofluorescence analysis of synapsin I and PSD95 in CA1, CA3, DG, and PFC regions of each group. Scale bar: 100 μm. Error bars signify mean ± SEM ($n = 4$–6 animals per group). $^{###}P < 0.001$, $^{####}P < 0.0001$ *vs.* control; $^{**}P < 0.01$ *vs.* model.

inflammatory factors. Behavioral tests revealed that compound HXY14 alleviated memory deficits and improved cognitive performance in Aβ_{1-42}-induced AD mice. Serum biochemical indices and hippocampal morphological examinations demonstrated its favorable safety profile *in vivo*. Notably, mechanistic investigations further revealed that the sEH inhibitor HXY14 markedly attenuated neuroinflammation and microglial activation in AD models. In addition, HXY14 enhanced neuroprotective effects and mitigated synaptic dysfunction in AD mice, contributing significantly to the cognitive improvement in AD treatment. Collectively, *Excoecaria agallocha* L.-derived compound HXY14 exerts its anti-AD effects, thereby playing a pivotal role in the development of sEH inhibitors as a novel therapeutic strategy for AD.

Declaration of competing interest

The authors declare that they have no known competing financial interests or personal relationships that could have appeared to influence the work reported in this paper.

CRediT authorship contribution statement

Fan Yang: Writing – original draft, Formal analysis, Data curation. **Tingting Fu:** Writing – original draft, Formal analysis, Data curation. **Wandi Xiong:** Writing – review & editing, Writing – original draft, Data curation. **Shuting Zhang:** Visualization, Methodology, Formal analysis. **Junjie Wang:** Visualization, Formal analysis. **Wenjun Shan:** Methodology, Formal analysis. **Xinyi Chen:** Methodology, Formal analysis. **Mingbin Chen:** Methodology, Investigation. **Qi Guo:** Visualization. **Jinzhuo Li:** Validation, Data curation. **Junyi Li:** Data curation. **Jingru Liu:** Formal analysis. **Jin Liu:** Validation, Methodology. **Yong Rao:** Visualization, Validation. **Zhongping Jiang:** Writing – review & editing, Funding acquisition. **Congjun Xu:** Writing – review & editing, Writing – original draft, Supervision, Investigation, Funding acquisition, Conceptualization. **Ling Huang:** Writing – review & editing, Validation, Supervision, Funding acquisition, Conceptualization.

Acknowledgments

This work was financially supported by the National Natural Science Foundation of China (No. 82204193 to C. Xu; No. 82204275 to Z. Jiang; No. 82404601 to W. Xiong; No. 82160653 to L. Huang) and Excellent Talent Team Project in Hainan Province (No. HNYT20250004).

Supplementary materials

Supplementary material associated with this article can be found, in the online version, at doi:10.1016/j.cclet.2025.111773.

References

[1] Alzheimer's Association, Alzheimer Dement. 21 (2025) e70235.
[2] S. Kamaljeet, G.D. Singh, K.R. Gupta, et al., Pharm. Sci. Adv. 2 (2024) 100021.
[3] R.R. Lin, H.F. Huang, Q.Q. Tao, Innovation Med. 1 (2023) 100020.
[4] P.B. Gonçalves, A.C.R. Sodero, Y. Cordeiro, Eur. J. Med. Chem. 276 (2024) 116684.

[5] B.K. Beata, J. Wojciech, K. Johannes, L. Piotr, M. Barbara, Int. J. Mol. Sci. 24 (2023) 1059.
[6] G.D. Stanciu, A. Luca, R.N. Rusu, et al., Biomolecules 10 (2019) 40.
[7] J. Zhang, C. Liu, J. Lü, R. Xu, W. Le, Innovation Life 2 (2024) 100084.
[8] J. Gu, J. Gu, L. Yu, Chin. Chem. Lett. 36 (2025) 110727.
[9] J. Zhang, Y. Zhang, J. Wang, et al., Signal Transduct. Targeted Ther. 9 (2024) 211.
[10] W. Li, M.J. Dong, H. Dai, et al., Chin. Chem. Lett. 36 (2025) 110614.
[11] Y. Jiang, Z. Zeng, J. Yao, et al., Chin. Chem. Lett. 34 (2023) 107966.
[12] B. Turgutalp, C. Kizil, Trends Pharmacol. Sci. 45 (2024) 628–638.
[13] 2024 Alzheimer's disease facts and figures, Alzheimer Dement. 20 (2024) 3708–3821.
[14] H. Fillit, A. Green, Nat. Rev. Neurol. 17 (2021) 129–130.
[15] C. Scuderi, R. Facchinetti, L. Steardo, M. Valenza, FASEB J. 34 (2020) 1.
[16] P. Ghosh, R. Singh, A. Ganeshpurkar, et al., Neurochem. Int. 151 (2021) 105212.
[17] D. Kaur, V. Sharma, R. Deshmukh, Inflammopharmacology 27 (2019) 663–677.
[18] J. Capdevila, L.J. Marnett, N. Chacos, R.A. Prough, R.W. Estabrook, Proc. Natl. Acad. Sci. U. S. A. 79 (1982) 767–770.
[19] N. Chacos, J.R. Falck, C. Wixtrom, J. Capdevila, Biochem. Biophys. Res. Commun. 104 (1982) 916–922.
[20] J.D. Imig, B.D. Hammock, Nat. Rev. Drug Discov. 8 (2009) 794–805.
[21] T.R. Harris, B.D. Hammock, Gene 526 (2013) 61–74.
[22] K.M. Wagner, C.B. McReynolds, W.K. Schmidt, B.D. Hammock, Pharmacol. Ther. 180 (2017) 62–76.
[23] J. Ding, M.Z. Zhu, X.Y. Du, et al., J. Med. Chem. 68 (2025) 8980–9013.
[24] C.P. Sun, X.Y. Zhang, C. Morisseau, et al., J. Med. Chem. 64 (2021) 184–215.
[25] C. Griñán-Ferré, S. Codony, E. Pujol, et al., Neurotherapeutics 17 (2020) 1825–1835.
[26] C.C. Hung, Y.H. Lee, Y.M. Kuo, et al., J. Neuroinflammation 16 (2019) 123.
[27] H.T. Lee, K.I. Lee, C.H. Chen, T.S. Lee, J. Neuroinflammation 16 (2019) 267.
[28] A. Ghosh, M.M. Comerota, D. Wan, et al., Sci. Transl. Med. 12 (2020) 573.
[29] D. Chen, R. Whitcomb, E. MacIntyre, et al., J. Clin. Pharmacol. 52 (2012) 319–328.
[30] A.L. Lazaar, L. Yang, R.L. Boardley, et al., Br. J. Clin. Pharmacol. 81 (2016) 971–979.
[31] B.D. Hammock, C.B. McReynolds, K. Wagner, et al., J. Med. Chem. 64 (2021) 1856–1872.
[32] Z. Li, Z. Zhang, B. Yu, J. Med. Chem. 68 (2025) 2377–2402.
[33] A.G. Atanasov, S.B. Zotchev, V.M. Dirsch, et al., Nat. Rev. Drug Discov. 20 (2021) 200–216.
[34] Z.B. Liu, C.P. Sun, J.X. Xu, et al., Int. J. Biol. Macromol. 133 (2019) 1187–1193.
[35] N.P. Thao, B.T.T. Luyen, J.S. Lee, et al., J. Nat. Prod. 80 (2017) 1867–1875.
[36] C.Y. Wang, L. Sunggun, J. Hyun-Jae, et al., J. Enzyme Inhib. Med. Chem. 34 (2019) 753–760.
[37] Y.F. Shao, Q.X. Huang, J.Y. Li, et al., Chem. Biodivers. 22 (2025) e202500013.
[38] J.Y. Li, M.B. Chen, Y. Rao, Z.P. Jiang, L. Huang, Chin. J. Org. Chem. 44 (2024) 3526–3530.
[39] J.Y. Li, M.B. Chen, T.T. Fu, et al., Phytochemistry 234 (2025) 114440.
[40] F. Du, R. Cao, L. Chen, et al., Acta Pharm. Sin. B 12 (2022) 1377–1389.
[41] F. Du, W. Sun, C. Morisseau, et al., Eur. J. Med. Chem. 223 (2021) 113678.
[42] Y. Chen, L. Chen, H. Xu, et al., J. Med. Chem. 66 (2023) 2979–3009.
[43] G.A. Gomez, C. Morisseau, B.D. Hammock, D.W. Christianson, Protein Sci. 15 (2006) 58–64.
[44] X. He, W.Y. Zhao, B. Shao, et al., Int. J. Biol. Macromol. 158 (2020) 1362–1368.